

Dynamic Token Reduction during Generation for Vision Language Models

Xiaoyu Liang^{*1}, Chaofeng Guan^{*1}, Jiaying Lu¹, Huiyao Chen², Huan Wang³, and Haoji Hu^{†1}

¹Zhejiang University, Hangzhou, China

²Harbin Institute of Technology, Shenzhen, China

³Westlake University, Hangzhou, China

Abstract—Vision-Language Models (VLMs) have achieved notable success in multimodal tasks but face practical limitations due to the quadratic complexity of decoder attention mechanisms and autoregressive generation. Existing methods like FASTV [1] and VTW [2] have achieved notable results in reducing redundant visual tokens, but these approaches focus on pruning tokens in a single forward pass without systematically analyzing the redundancy of visual tokens throughout the entire generation process. In this paper, we introduce a dynamic pruning strategy tailored for VLMs, named Dynamic Rate (DyRate), which progressively adjusts the compression rate during generation. Our analysis of the distribution of attention reveals that the importance of visual tokens decreases throughout the generation process, inspiring us to adopt a more aggressive compression rate. By integrating a lightweight predictor based on attention distribution, our approach enables flexible adjustment of pruning rates based on the attention distribution. Our experimental results demonstrate that our method not only reduces computational demands but also maintains the quality of responses.

Index Terms—Multimodal, Token Pruning, Compression

I. INTRODUCTION

Vision-Language Models (VLMs) integrate visual and textual information to generate coherent and contextually relevant outputs, demonstrating impressive capabilities across various tasks in artificial intelligence [3]–[5]. However, the autoregressive generation nature of VLMs, along with the quadratic complexity of attention [6], significantly increases computational complexity when the input token sequence lengthens, limiting the applications of VLMs.

Many recent methods attempt to reduce the computational cost by eliminating redundant visual tokens. For example, FastV [1] analyzes the attention mechanism and discovers that visual tokens receive less attention after the second decoder layers, thus deleting redundant visual tokens according to a predefined compression rate. Building on this observation, VTW [2] directly removes all visual tokens in deeper layers, only text tokens allowed to participate in further processing.

Although these methods demonstrate effectiveness, they still present two drawbacks. *First*, the compression rate must be manually specified. Manually selecting an appropriate compression rate is nontrivial and typically requires expert-level domain knowledge. *Second*, maintaining a fixed compression

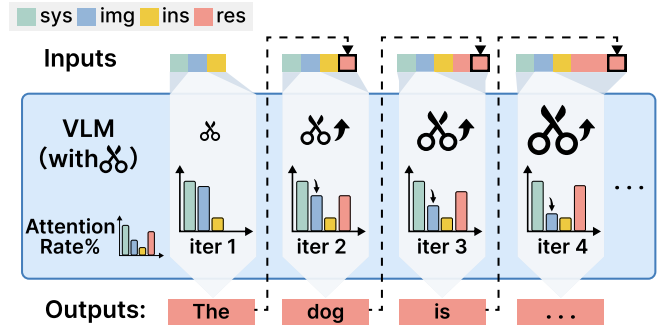


Fig. 1. As the VLMs continue to generate, the attention proportions among the four token types (system, image, instruction, response) fluctuate. Notably, as the number of iterations increases, visual tokens receive decreasing attention. This observation suggests that we can adjust the appropriate compression rate R based on the attention distribution to implement more aggressive pruning during the model’s generation process.

rate during the generation process is suboptimal. Our experimental analyses of the attention distribution during generation (see Sec. III-A) reveal that visual tokens receive varying proportions of attention during the next token prediction. Information in VLMs often becomes less concentrated in visual tokens during the later iteration of generation. As the generation process advances and the length of the response gradually increases, the importance of the visual information changes accordingly. Thus, it is imperative to have *adaptive* compression rates during generation. Yet, determining proper compression rates is challenging. Our work is here to address the challenge.

We present **Dynamic Rate (DyRate)**, the *first* method to connect the token reduction rate with the attention weights to achieve adaptive dynamic reduction during the VLM generation process. Our approach is designed to be *differentiable*, enabling end-to-end training. Specifically, we introduce a lightweight classifier to predict the reduction rate. During each iteration of model generation, we collect the attention distributions of four types of tokens in each head, which are then fed into the predictor to determine the optimal reduction rate for cropping the image embeddings. The overview of our approach is shown in Fig. 1. Our contributions are summarized as follows:

- we propose DyRate, the *first* approach that can adaptively

^{*}These authors contributed equally to this work.

[†]Corresponding author.

- adjust the token reduction rate during model generation.
- ★ we present an effective training strategy based on Gumbel-Softmax which enables end-to-end training of our proposed module;
 - ★ through extensive experiments, we demonstrate the effectiveness of our approach in maintaining accuracy while reducing computational demands.

II. RELATED WORK

A. Efficient VLMs

The computational demands of VLMs increase significantly with long token sequences due to the quadratic complexity of attention mechanisms. This limitation restricts their application in tasks such as high-resolution image understanding [7] and video understanding [8]. To address this issue, prior research has proposed several strategies. For instance, MoE-Llava [9] integrates a Mixture of Experts framework to accelerate the model, while VL-Mamba [10] explores alternative architectures to enhance efficiency. Another approach involves using smaller language models, such as LLaVA-Phi [11] and mobileVLM [12], which demonstrate efficiency with minimal performance loss. Additionally, compression techniques like pruning [13], quantization [14], [15], and knowledge distillation [16] are widely used to reduce the number of parameters in models.

However, these methods often require modifications to the model architecture or parameters, complicating further development. In contrast, token reduction minimizes token sequences without altering the model architecture, addressing the quadratic complexity of VLMs. Token reduction has been extensively explored and validated within encoder architectures like ViT and BERT, primarily through pruning [17]–[19] and merging [20]–[22] strategies.

B. Token Reduction for VLMs

Recent researchers have applied token reduction methods to VLMs, categorizing them based on the architecture of VLMs. For the visual encoder, methods like LLaVA-PruMerge [23] and MADTP [24] introduce adaptive methods to reduce visual tokens, significantly decreasing their number while maintaining comparable performance to the original models. In the cross-modality projector, Tokenpacker [25] optimizes the bridge between textual and visual information to minimize the number of visual tokens. FastV [1], SparseVlm [26] and Visionzip [27] removes redundant visual tokens during the inference phase to reduce computational demands without impacting performance. VTW [2] observes that visual tokens are not significant in deeper layers of the VLM and strategically removes all visual tokens from specific layers, allowing only text tokens to proceed in subsequent processing.

Although existing token reduction methods improve the efficiency of inference, they often overlook the autoregressive nature of VLM decoders. Our work addresses this gap by dynamically adjusting R based on the changing attention distribution during the generation process.

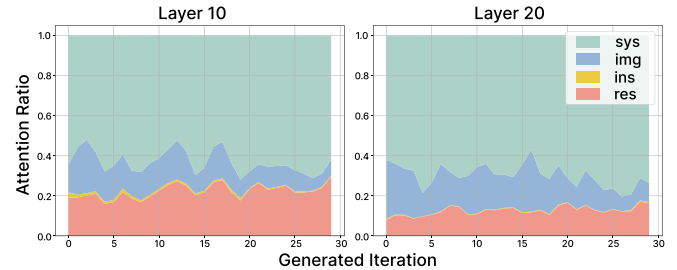


Fig. 2. **Attention stack per iteration** during the decoding process of LLaVA1.5-7B on the Flickr30K [28] dataset, the x-axis represents the time step in generations. The left graph depicts shallow layers, while the right graph represents deep layers. Our findings indicate that as generations progress, the importance of visual tokens gradually decreases. We categorize the input tokens at each iteration into four types: system prompt (sys), image token (img), user instruction (ins), and response token (res).

III. METHODS

In Sec. III-A, we explore how attention distribution changes during the generation within VLMs. Our analysis reveals that the importance of visual tokens gradually decreases as the VLM progresses. This observation leads us to question whether the fixed compression rate R set manually in previous works [1], [2] is the optimal solution, considering the changing attention distribution.

Based on this insight, we propose DyRate as a solution to adjust the compression rate R . The overall process is illustrated in Fig. 3.

A. Visual Redundancy during Generation

We observed that visual token redundancy increases with generation steps. In Fig. 2, as the model generates more tokens, it emphasizes response tokens and overlooks visual tokens, indicating increasing redundancy.

According to information flow theory [29], a large amount of information from image tokens is aggregated into response tokens during generation. The aggregation of this information results in additional redundancy among visual tokens, where a large number of tokens provide minimal information, leading to a waste of computational resources.

Given the above, a fixed R fails to adapt to the changing attention distribution during the generation process, highlighting the need to determine an adaptive R .

B. Token Reduction with Prediction Module

To address this issue, we first intuitively hypothesize that the redundancy of visual tokens is closely related to the attention distribution across four different token types. At each time step of the model generation, we compute the attention distribution for each attention head. Based on these distribution characteristics, we further train a linear classifier aimed at identifying and determining the optimal token pruning rate R . The entire process is depicted in Figure 3.

During training, we use the mask M to selectively prune tokens, while during inference, we discard tokens directly to save computational resources. It's worth to note that the

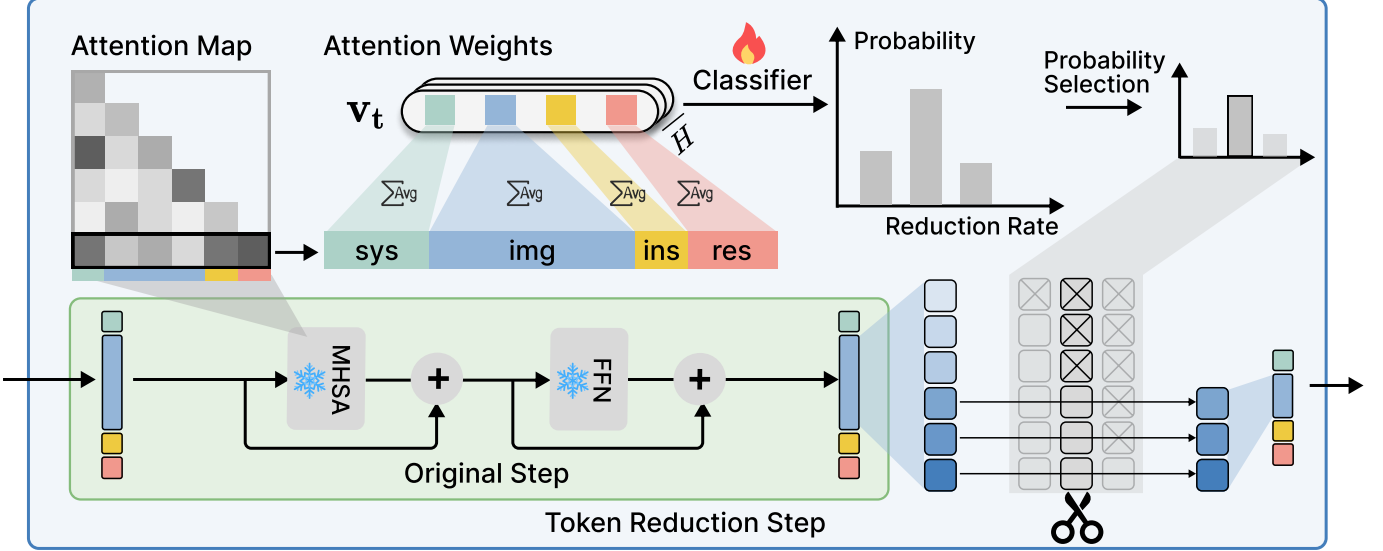


Fig. 3. The pipeline of our method. We calculate the attention distribution for each attentional head and train a linear classifier to find the optimal token pruning rate R . The classifier can be trained end-to-end.

FLOPs required by the predictor is minimal when compared to the computational savings gained from discarding these tokens.

C. Differentiable Compression Rate

To effectively address the non-differentiability issues associated with sampling and masking operations, we utilize the Gumbel-Softmax trick [17], [20], [30] to convert the probability distribution of the compression rate R predicted by the predictor C into a differentiable mask probability distribution, which is then integrated into the forward propagation of the model.

1) *Probability of Pruning Rate*: We define the adjustment of the compression rate R as a classification problem, and discretize the compression rate R into K discrete values:

$$\mathcal{R} = \{r_k\}_{k=1}^K, \quad (1)$$

where $r_k = \frac{k-1}{K}$ represents removing $\frac{(k-1) \cdot N}{K}$ less important tokens in a token sequence of length N . Note that $r_1 = 0$ indicates retaining all tokens.

We feed the vector v_t to classifier C to predict the probability distribution over these rates:

$$\pi_R = \text{Softmax}(C_\theta(v_t)) = \{P(r_k)\}_{k=1}^K, \quad (2)$$

where the probabilities sum to one and are differentiable.

Specifically, we sort the tokens based on the ‘attention-score’ rule utilized in FastV [1]. After that, we apply masks at different pruning rates:

$$m_i^k = \begin{cases} 1 & \text{if } i \leq \frac{N}{K}(k-1), \\ 0 & \text{otherwise,} \end{cases} \quad (3)$$

where 0 indicates an unimportant token to be discarded, and 1 indicates a token to be retained. For each potential R_i , we

generate a unique corresponding mask M_i , ensuring that the least important tokens are discarded first.

2) *Gumbel-Softmax Sampling*: During the forward pass, Gumbel-Softmax generates a one-hot vector with the same expectation as π_R :

$$R = \text{Gumbel-Softmax}(\pi_R) \in \{0, 1\}^K, \quad (4)$$

where their parameter gradients can be easily computed with standard backpropagation. During the backward pass, the straight-through Gumbel-Softmax estimator is employed to approximate the gradient.

We can then select current mask M by sampling from π :

$$m = \sum_{k=1}^K \text{Gumbel-Softmax}(\pi_R)_{*,k} \cdot m^k, \quad (5)$$

where $m_k \in \{0, 1\}^N$ is the mask associated with the discrete compression rate r_k .

This generates the final mask $M \in \{0, 1\}^{N \times N}$, which, in conjunction with the causal mask, is applied to the attention computation to achieve token pruning.

$$M_{i,j} = \begin{cases} 1 & i = j, \\ m_i & i \neq j. \end{cases} \quad (6)$$

The process ensures that the selection operation remains differentiable with respect to R . And we keep the proof and pseudocode for our DyRate algorithm in the Appendix.

IV. EXPERIMENTS

A. Settings

We utilized LLaVA-1.5-7B and LLaVA-1.5-13B models, where visual inputs were represented using 576 tokens. To evaluate the general performance of our proposed method,

TABLE I
COMPARISON AMONG DIFFERENT VLMs ON 4 VISUAL QUESTION ANSWERING BENCHMARKS AND 3 COMMON BENCHMARKS. BENCHMARK NAMES ARE ABBREVIATED DUE TO SPACE LIMITS. THE HIGHEST-PERFORMING RESULTS ARE HIGHLIGHTED IN **BOLDFACE**.

Model	LLM	Res.	Visual Question Generation				Short Generation		
			GQA↑ <i>EM</i>	VisWiz↑ <i>EM</i>	SQA↑ <i>EM</i>	VQA ^T ↑ <i>EM</i>	POPE↑ Accuracy	MMB↑ Accuracy	MME↑ Accuracy
InstructBLIP	Vicuna-7B	224	49.2	34.5	60.5	50.1	79.8	36.0	–
InstructBLIP	Vicuna-13B	224	49.5	33.4	63.1	50.7	78.9	–	1212.8
MiniGPT-4	Vicuna-13B	224	41.0	19.6	61.0	42.5	85.3	–	1293.8
Qwen-VL	Qwen-7B	448	59.3	35.2	67.1	63.8	–	38.2	–
Qwen-VL-Chat	Qwen-7B	448	57.5	38.9	68.2	61.5	–	60.6	1487.5
LLaMA-VID	Vicuna-7B	336	64.3	54.1	68.3	–	86.0	63.4	1521.4
VoCo-LLaMA	Vicuna-7B	33	57.0	53.0	65.4	52.7	81.4	58.8	1323.3
TokenPacker	Vicuna-7B	336	61.9	52.0	–	–	87	65.1	–
M ³	Vicuna-7B	336	61.3	53.1	67.2	–	86.6	63.6	–
PruMerge	Vicuna-7B	336	61.8	53.5	68.5	56.0	76.3	60.9	1350.3
LLaVAv1.5	Vicuna-7B	336	62.0	50.0	66.8	58.2	85.9	64.3	1510.7
FastV	Vicuna-7B	336	60.3	54.4	69.0	45.4	82.5	63.9	1510.2
VTW	Vicuna-7B	336	55.1	50.9	69.1	16.1	85.9	64.0	1501.4
SparseVLM	Vicuna-7B	336	57.6	–	69.1	56.1	83.6	62.5	1721
VisionZip	Vicuna-7B	336	60.1	–	68.9	57.1	84.93	63.4	1834
DyRate(ours)	Vicuna-7B	336	61.9	54.2	69.2	45.7	86.8	64.1	1516.6

TABLE II
CIDER SCORES OF DIFFERENT METHODS ON NOCAPS, FLICKR30K, AND COCO2017 DATASETS.

Models	Methods	Nocaps↑ <i>CIDEr</i>	Flickr30k↑ <i>CIDEr</i>	COCO2017↑ <i>CIDEr</i>
LLaVA-1.5 -7B	Original	74.89	105.57	110.43
	FastV _(K=3,R=0.5)	74.75	105.00	110.80
	FastV _(K=2,R=0.5)	74.86	104.00	110.40
	VTW _(K=16,R=1)	44.54	58.00	67.20
	DyRate(ours)	75.00	108.41	110.54
LLaVA-1.5 -13B	Original	109.31	79.56	115.57
	FastV _(K=3,R=0.5)	102.70	73.40	105.36
	FastV _(K=2,R=0.5)	103.10	73.40	108.85
	VTW _(K=16,R=1)	95.21	65.87	101.67
	DyRate(ours)	113.23	79.38	115.72

we conducted comparisons with existing models and mainstream token compression techniques across seven widely-used benchmarks. Additionally, we employed three long-response tasks to simulate its capabilities in daily conversation.

We conducted systematic evaluations of the model’s performance across multiple datasets using the LMM-Eval evaluation framework on eight NVIDIA GeForce RTX 4090 GPUs. More details in Appendix.

B. Main Results

1) *Short Responses*: Our model demonstrated exceptional performance on short-response datasets, showcasing superior question comprehension and answer generation capabilities. It performed particularly well on the Flickr30K and GQA datasets and handled specific query types well on the SQA[1] and VisWiz datasets. Notably, performance remained stable across different datasets, even under high compression rates,

although a minor performance drop was observed during detailed visual analysis tasks.

2) *Long Responses*: With long-response datasets, our model’s strategy of gradually adjusting the pruning ratio during autoregressive generation effectively reduced redundancy. Despite reducing visual tokens by half, the model maintained high performance across multiple datasets. This strategy proved especially beneficial for generating long responses and managing high redundancy data, all while requiring less computational resources.

C. Efficiency

We are also concerned with the performance of our method in scenarios involving long responses, as such situations frequently arise in real-life applications. Therefore, we selected the Flickr30K, COCO2017 and Nocaps dataset for evaluation. These datasets feature response token lengths ranging from 16 to 64 tokens, providing a comprehensive basis for evaluating the comprehension abilities of VLMs and the effects of post-token pruning. For a fair comparison, we evaluated the performance of two highly relevant methods, FastV and VTW under scenarios with FLOPs savings ratio of 30% and 50%.

The experimental results demonstrate that our method, DiffRate, effectively meets FLOPs resource constraints by automatically optimizing the parameter R, eliminating the need for manual searching. This adaptive approach to R proves to be more effective. For ease of comparison with FastV, we selected the same number of layers.

D. Ablation

1) *Compression Rate Strategies*: Our ablation studies explored the effects of different pruning strategies on Visual Language Models (VLM) performance. We compared

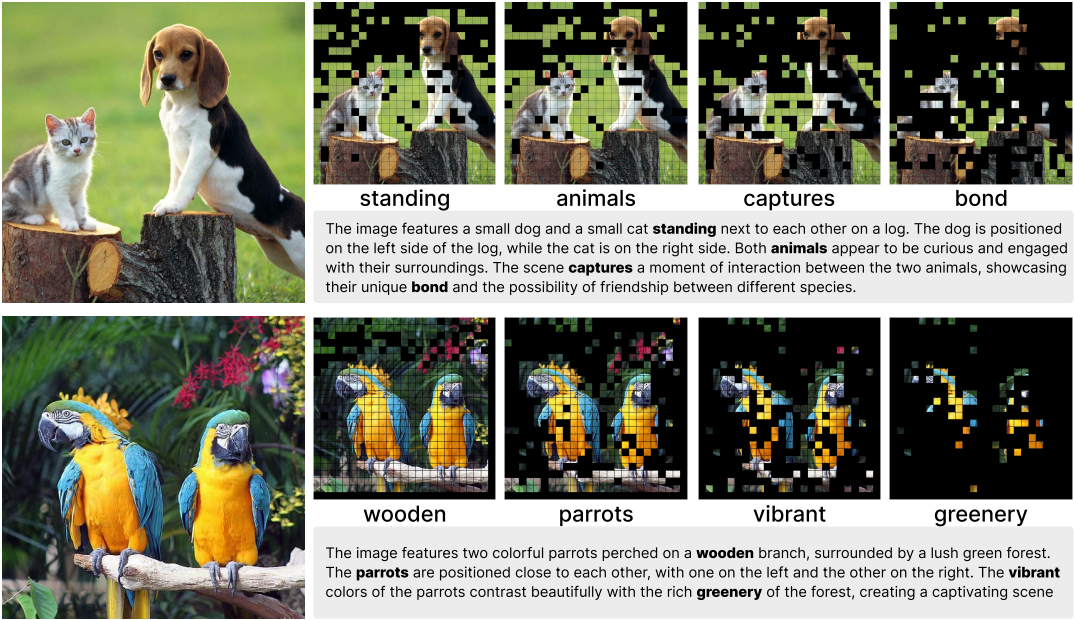


Fig. 4. We explore the mask of the image for each token iteration in the model generation process.

TABLE III
COMPARING TOKEN REDUCTION METHODS FOR COMPLEX SCENE DESCRIPTION.

Methods	TFLOPs(%) \downarrow	Latency (ms) \downarrow	Nocaps \uparrow	Auto R
LLaVA-1.5-7B				
Original	100.0	70.80	74.89	\times
FastV $_{(K=3,R=0.5)}$	57.90	42.36	74.75	\times
FastV $_{(K=2,R=0.5)}$	55.40	41.37	74.86	\times
VTW $_{(K=16,R=1)}$	55.20	46.24	44.54	\times
DyRate(ours)	33.33	40.13	75.00	\checkmark
LLaVA-1.5-13B				
Original	100.0	128.36	109.31	\times
FastV $_{(K=3,R=0.5)}$	57.90	73.35	102.70	\times
FastV $_{(K=2,R=0.5)}$	55.40	72.25	103.10	\times
VTW $_{(K=16,R=1)}$	55.20	80.78	95.21	\times
DyRate(ours)	33.33	65.16	113.23	\checkmark

TABLE IV
ABLATION EXPERIMENTS FOR LLaVA1.5-7B ON NOCAPS DATASET.

(a) Generation Type		(b) Pruning Strategy		
Strategy	Nocaps \uparrow <i>CIDEr</i>	Strategy	Nocaps \uparrow <i>CIDEr</i>	FLOPs \downarrow (%)
Greedy	106.74	LLaVA	105.57	100.00
Beam-2	109.06	FastV	105.00	57.90
Beam-5	108.28	Ours(FP)	107.00	28.80
top_p	109.57	Ours(DP)	105.00	58.10

FixedPrune(FP), a strategy with a static pruning ratio, and DepthBasedPrune(DP), a strategy with a dynamically adjusted pruning ratio based on layer depth. These strategies were evaluated on the NoCaps dataset, using $K = 3$ layers for pruning, in line with FastV for a valid comparison.

Our innovative strategy for determining R was as follows:

$$C_{\text{retain}} = 1 - H(L_{\text{index}} - 4) \cdot P_{\text{prune_4th}} - H(L_{\text{index}} - 4) \cdot R'$$

Here, C_{retain} denoted the proportion of visual tokens kept in the current layer, L_{index} represented the current layer index, $P_{\text{prune_4th}}$ was the fourth layer's pruning ratio, and R' was a modified pruning ratio adapting to the layer index.

The results showed that our method efficiently met Floating Point Operations Per Second (FLOPs) resource constraints without manual search, indicating the effectiveness of the adaptive R .

2) *Decoding Parameters*: We also investigated how decoding strategies impacted VLM generation. Adjusting a single decoding parameter in LLaVA-1.5 while fixing others revealed the significant effect of decoding parameters on the quality of generated text. Particularly, setting top_k to 6 resulted in the best performance, with a CIDEr score of '109.57'. To maintain fairness, we used LLaVA-1.5 with the default greedy search for replication, thereby reducing the influence of other parameters.

E. Visualization

To comprehensively elucidate the functioning of our proposed method, we visualized the alterations in image masking throughout the generation process in Figure 4. We employed a diverse collection of original images and introduced them to the LLaVA-1.5-7B model with the prompt: 'Provide a one-sentence caption for the provided image.' As the generation iterations escalate, we document an associated increase in the cropping ratio. This trend suggests that the model incrementally diminishes its attention on redundant information within the image during the generation, honing in on the extraction and processing of pivotal information. Additionally, by contrasting the generation trajectories of different images,

we discern that our method exhibits flexibility in adapting to images of assorted types and complexities, reinforcing the efficacy and robustness of our proposed approach.

V. CONCLUSION

This paper introduces a novel method, **Dynamic Rate (DyRate)**, to dynamically determine compression rate R for VLMs during the generation process. Our approach leverages a lightweight predictor that utilizes the attention distribution across different token types to identify the most effective compression rate, thereby addressing the computational inefficiencies associated with fixed compression rates. We employ Gumbel-Softmax to overcome the non-differentiability challenges associated with traditional pruning methods. The empirical validation across multiple benchmarks underscores the effectiveness of our method in maintaining accuracy while reducing computational demands. This study not only enhances the efficiency of VLMs, but also paves the way for more adaptable and resource-aware applications in complex multimodal environments.

REFERENCES

- [1] Liang Chen, Haozhe Zhao, Tianyu Liu, Shuai Bai, Junyang Lin, Chang Zhou, and Baobao Chang, “An image is worth 1/2 tokens after layer 2: Plug-and-play inference acceleration for large vision-language models,” *CoRR*, vol. abs/2403.06764, 2024.
- [2] Zhihang Lin, Mingbao Lin, Luxi Lin, and Rongrong Ji, “Boosting multimodal large language models with visual tokens withdrawal for rapid inference,” *CoRR*, vol. abs/2405.05803, 2024.
- [3] Jinze Bai, Shuai Bai, Shusheng Yang, Shijie Wang, Sinan Tan, Peng Wang, Junyang Lin, Chang Zhou, and Jingren Zhou, “Qwen-vl: A frontier large vision-language model with versatile abilities,” *arXiv preprint arXiv:2308.12966*, 2023.
- [4] Bin Lin, Bin Zhu, Yang Ye, Munan Ning, Peng Jin, and Li Yuan, “Video-llava: Learning united visual representation by alignment before projection,” *arXiv preprint arXiv:2311.10122*, 2023.
- [5] Shilong Liu, Hao Cheng, Haotian Liu, Hao Zhang, Feng Li, Tianhe Ren, Xueyan Zou, Jianwei Yang, Hang Su, Jun Zhu, et al., “Llava-plus: Learning to use tools for creating multimodal agents,” *arXiv preprint arXiv:2311.05437*, 2023.
- [6] Zixuan Zhou, Xuefei Ning, Ke Hong, Tianyu Fu, Jiaming Xu, Shiyao Li, Yuming Lou, Luning Wang, Zhihang Yuan, Xiuhong Li, Shengen Yan, Guohao Dai, Xiao-Ping Zhang, Yuhan Dong, and Yu Wang, “A survey on efficient inference for large language models,” *CoRR*, vol. abs/2404.14294, 2024.
- [7] Yi-Fan Zhang, Qingsong Wen, Chaoyou Fu, Xue Wang, Zhang Zhang, Liang Wang, and Rong Jin, “Beyond llava-hd: Diving into high-resolution large multimodal models,” *CoRR*, vol. abs/2406.08487, 2024.
- [8] Hang Zhang, Xin Li, and Lidong Bing, “Video-llama: An instruction-tuned audio-visual language model for video understanding,” in *Proceedings of the 2023 Conference on Empirical Methods in Natural Language Processing, EMNLP 2023 - System Demonstrations, Singapore, December 6-10, 2023*, Yansong Feng and Els Lefever, Eds. 2023, pp. 543–553, Association for Computational Linguistics.
- [9] Bin Lin, Zhenyu Tang, Yang Ye, Jiaxi Cui, Bin Zhu, Peng Jin, Junwu Zhang, Munan Ning, and Li Yuan, “Moe-llava: Mixture of experts for large vision-language models,” *CoRR*, vol. abs/2401.15947, 2024.
- [10] Yanyuan Qiao, Zheng Yu, Longteng Guo, Sihan Chen, Zijia Zhao, Mingzhen Sun, Qi Wu, and Jing Liu, “VI-mamba: Exploring state space models for multimodal learning,” *CoRR*, vol. abs/2403.13600, 2024.
- [11] Yichen Zhu, Minjie Zhu, Ning Liu, Zhicai Ou, Xiaofeng Mou, and Jian Tang, “Llava-phi: Efficient multi-modal assistant with small language model,” *CoRR*, vol. abs/2401.02330, 2024.
- [12] Xiangxiang Chu, Limeng Qiao, Xinyang Lin, Shuang Xu, Yang Yang, Yiming Hu, Fei Wei, Xinyu Zhang, Bo Zhang, Xiaolin Wei, and Chunhua Shen, “Mobilevlm : A fast, strong and open vision language assistant for mobile devices,” *CoRR*, vol. abs/2312.16886, 2023.
- [13] Xinyin Ma, Gongfan Fang, and Xinchao Wang, “Llm-pruner: On the structural pruning of large language models,” in *Advances in Neural Information Processing Systems 36: Annual Conference on Neural Information Processing Systems 2023, NeurIPS 2023, New Orleans, LA, USA, December 10 - 16, 2023*, Alice Oh, Tristan Naumann, Amir Globerson, Kate Saenko, Moritz Hardt, and Sergey Levine, Eds., 2023.
- [14] Tim Dettmers, Mike Lewis, Younes Belkada, and Luke Zettlemoyer, “Llm.int8(): 8-bit matrix multiplication for transformers at scale,” *CoRR*, vol. abs/2208.07339, 2022.
- [15] Elias Frantar, Saleh Ashkboos, Torsten Hoefer, and Dan Alistarh, “GPTQ: accurate post-training quantization for generative pre-trained transformers,” *CoRR*, vol. abs/2210.17323, 2022.
- [16] Zhaorui Yang, Qian Liu, Tianyu Pang, Han Wang, Haozhe Feng, Minfeng Zhu, and Wei Chen, “Self-distillation bridges distribution gap in language model fine-tuning,” *CoRR*, vol. abs/2402.13669, 2024.
- [17] Yongming Rao, Wenliang Zhao, Benlin Liu, Jiwen Lu, Jie Zhou, and Cho-Jui Hsieh, “Dynamicvit: Efficient vision transformers with dynamic token sparsification,” in *Advances in Neural Information Processing Systems 34: Annual Conference on Neural Information Processing Systems 2021, NeurIPS 2021, December 6-14, 2021, virtual*, Marc'Aurelio Ranzato, Alina Beygelzimer, Yann N. Dauphin, Percy Liang, and Jennifer Wortman Vaughan, Eds., 2021, pp. 13937–13949.
- [18] Youwei Liang, Chongjian Ge, Zhan Tong, Yibing Song, Jue Wang, and Pengtao Xie, “Evit: Expediting vision transformers via token reorganizations,” in *The Tenth International Conference on Learning Representations, ICLR 2022, Virtual Event, April 25-29, 2022*, 2022, OpenReview.net.
- [19] Sehoon Kim, Sheng Shen, David Thorsley, Amir Gholami, Woosuk Kwon, Joseph Hassoun, and Kurt Keutzer, “Learned token pruning for transformers,” in *KDD ’22: The 28th ACM SIGKDD Conference on Knowledge Discovery and Data Mining, Washington, DC, USA, August 14 - 18, 2022*, Aidong Zhang and Huzeifa Rangwala, Eds. 2022, pp. 784–794, ACM.
- [20] Mengzhao Chen, Wenqi Shao, Peng Xu, Mingbao Lin, Kaipeng Zhang, Fei Chao, Rongrong Ji, Yu Qiao, and Ping Luo, “Diffrate : Differentiable compression rate for efficient vision transformers,” in *IEEE/CVF International Conference on Computer Vision, ICCV 2023, Paris, France, October 1-6, 2023*. 2023, pp. 17118–17128, IEEE.
- [21] Daniel Bolya, Cheng-Yang Fu, Xiaoliang Dai, Peizhao Zhang, Christoph Feichtenhofer, and Judy Hoffman, “Token merging: Your vit but faster,” in *The Eleventh International Conference on Learning Representations, ICLR 2023, Kigali, Rwanda, May 1-5, 2023*. 2023, OpenReview.net.
- [22] Jiarui Xu, Shalini De Mello, Sifei Liu, Wonmin Byeon, Thomas M. Breuel, Jan Kautz, and Xiaolong Wang, “Groupvit: Semantic segmentation emerges from text supervision,” in *IEEE/CVF Conference on Computer Vision and Pattern Recognition, CVPR 2022, New Orleans, LA, USA, June 18-24, 2022*. 2022, pp. 18113–18123, IEEE.
- [23] Yuzhang Shang, Mu Cai, Bingxin Xu, Yong Jae Lee, and Yan Yan, “Llava-prumerge: Adaptive token reduction for efficient large multimodal models,” *CoRR*, vol. abs/2403.15388, 2024.
- [24] Jianjian Cao, Peng Ye, Shengze Li, Chong Yu, Yansong Tang, Jiwen Lu, and Tao Chen, “MADTP: multimodal alignment-guided dynamic token pruning for accelerating vision-language transformer,” *CoRR*, vol. abs/2403.02991, 2024.
- [25] Wentong Li, Yuqian Yuan, Jian Liu, Dongqi Tang, Song Wang, Jianke Zhu, and Lei Zhang, “Tokenpacker: Efficient visual projector for multimodal llm,” *arXiv preprint arXiv:2407.02392*, 2024.
- [26] Yuan Zhang, Chun-Kai Fan, Junpeng Ma, Wenzhao Zheng, Tao Huang, Kuan Cheng, Denis Gudovskiy, Tomoyuki Okuno, Yohei Nakata, Kurt Keutzer, et al., “Sparsevlm: Visual token sparsification for efficient vision-language model inference,” *arXiv preprint arXiv:2410.04417*, 2024.
- [27] Senqiao Yang, Yukang Chen, Zhuotao Tian, Chengyao Wang, Jingyao Li, Bei Yu, and Jiaya Jia, “Visionzip: Longer is better but not necessary in vision language models,” *arXiv preprint arXiv:2412.04467*, 2024.
- [28] Bryan A. Plummer, Liwei Wang, Chris M. Cervantes, Juan C. Caicedo, Julia Hockenmaier, and Svetlana Lazebnik, “Flickr30k entities: Collecting region-to-phrase correspondences for richer image-to-sentence models,” in *2015 IEEE International Conference on Computer Vision, ICCV 2015, Santiago, Chile, December 7-13, 2015*. 2015, pp. 2641–2649, IEEE Computer Society.
- [29] Xiaofeng Zhang, Chen Shen, Xiaosong Yuan, Shaotian Yan, Liang Xie, Wenxiao Wang, Chaochen Gu, Hao Tang, and Jieping Ye, “From

- redundancy to relevance: Enhancing explainability in multimodal large language models,” *CoRR*, vol. abs/2406.06579, 2024.
- [30] Huiyao Chen, Xinxin Li, Meishan Zhang, and Min Zhang, “Semantic role labeling from Chinese speech via end-to-end learning,” in *Findings of the Association for Computational Linguistics ACL 2024*, Lun-Wei Ku, Andre Martins, and Vivek Srikumar, Eds., Bangkok, Thailand and virtual meeting, Aug. 2024, pp. 8898–8911, Association for Computational Linguistics.